RESEARCH ARTICLE

Unbalance between working memory task-activation and task-deactivation networks in epilepsy: Simultaneous EEG-fMRI study

Yun Qin[1,2] | Sisi Jiang[1] | Siwei Xiong[1] | Sipei Li[3] | Qiankun Fu[3] | Lili Yang[4] | Peishan Du[4] | Cheng Luo[1] | Dezhong Yao[1,2]

[1]The Clinical Hospital of Chengdu Brain Science Institute, MOE Key Lab for Neuroinformation, School of Life Science and Technology, University of Electronic Science and Technology of China, Chengdu, China

[2]Sichuan Institute for Brain Science and Brain-Inspired Intelligence, Chengdu, China

[3]Glasgow College, University of Electronic Science and Technology of China, Chengdu, China

[4]Sichuan Provincial People's Hospital, University of Electronic Science and Technology of China, Chengdu, China

Correspondence
Cheng Luo, The Clinical Hospital of Chengdu Brain Science Institute, MOE Key Lab for Neuroinformation, School of life Science and Technology, University of Electronic Science and Technology of China, Chengdu 611731, China.
Email: chengluo@uestc.edu.cn

Abstract

Working memory (WM) is a cognitive function involving emergent properties of theta oscillations and large-scale network interactions. The synchronization of WM task-related networks in the brain enhanced WM performance. However, how these networks regulate WM processing is not well known, and the alteration of the interaction among these networks may play an important role in patients with cognitive dysfunction. In this study, we used simultaneous EEG-fMRI to examine the features of theta oscillations and the functional interactions among activation/deactivation networks during the n-back WM task in patients with idiopathic generalized epilepsy (IGE). The results showed that there was more enhancement of frontal theta power along with WM load increase in IGE, and the theta power was positively correlated with the accuracy of the WM tasks. Moreover, fMRI activations/deactivations correlated with n-back tasks were estimated, and we found that the IGE group had increased and widespread activations in high-load WM tasks, including the frontoparietal activation network and task-related deactivation areas, such as the default mode network and primary visual and auditory networks. In addition, the network connectivity results demonstrated decreased counteraction between the activation network and deactivation network, and the counteraction was correlated with the higher theta power in IGE. These results indicated the important role of the interactions between activation and deactivation networks during the WM process, and the unbalance among them may indicate the pathophysiological mechanism of cognitive dysfunction in generalized epilepsy.

KEYWORDS
activation network, deactivation network, simultaneous EEG-fMRI, theta oscillation, working memory

1 | INTRODUCTION

Neural oscillations modulate local and interregional activity and contribute to information processing and cognitive performance (Buzsaki & Draguhn, 2004; Klimesch, 1999). Cognitive function, such as working memory (WM), comprises emergent properties of neural oscillations and large-scale network interactions (Sreenivasan et al., 2014). Previous studies have demonstrated that the reactivity

of theta bands (4–8 Hz) to various memory paradigms illuminated the cortico-cortical interactions needed in the case of increasing memory load (Johnson et al., 2018; Zakrzewska & Brzezicka, 2014). Strengthened theta power and widespread theta synchrony based on EEG recording have been shown to underlie enhanced memory load, as well as the performance of the WM task (Hsieh & Ranganath, 2014; Toth et al., 2012). In patients with cognitive decline, impaired theta oscillation and brain connectivity were exhibited during WM processing (Missonnier et al., 2006; Sarnthein et al., 2005). The theta response over frontal regions increased network efficiency, primarily reflecting the activation of neural networks involved in the allocation of attention and attention control, thus playing an important role in directing local activity and long-range interactions during information processing in WM (Deiber et al., 2007; Rutishauser et al., 2010).

Frontal and parietal brain regions support WM processing (Cohen et al., 1997; Todd & Marois, 2004), and regulation among frontoparietal and frontotemporal networks modulates spatio-temporal dynamics and enhances WM performance (Klingberg et al., 1997; Violante et al., 2017). Therefore, the frontoparietal network is widely thought to be the task-activation network in WM. In addition, the default mode network (DMN) arising from resting-state fMRI, which showed great deactivation in WM, also demonstrated interaction with the WM activation network and facilitated WM performance (Koshino et al., 2014; Xin & Lei, 2015). Therefore, it was suggested that the existence of modulation between task-activation and task-deactivation brain networks played an important role in WM processing (Koshino et al., 2014; Newton et al., 2011). However, how the connectivity between task-activation and deactivation networks modulates WM processing, and the relationship between these networks and theta oscillation are still unknown.

The impairment of WM has been reported in local epilepsy, such as temporal lobe epilepsy and frontal lobe epilepsy (Santana et al., 2006; Stretton et al., 2012), as well as in generalized epilepsy (Myatchin et al., 2009; Swartz et al., 1996), which is a common epileptic subtype involving distributed altered activity and network connectivity in the brain. The altered representations of functional networks relative to WM in generalized epilepsy have not yet been fully investigated. In fact, dysfunction of the frontal and parietal regions is a key element contributing to discharge generation and propagation (Bai et al., 2010; Lee et al., 2014; Vaudano et al., 2009), while these regions are also involved in working memory networks (WMNs). Moreover, aberrant activity and functional connectivity in the DMN, which is a task-deactivation network in WM, play an important role in brain dysfunction and discharge activity in epilepsy (Gotman et al., 2005; Luo et al., 2011; Qin et al., 2019). Additionally, diffuse and hypersynchronous theta oscillation was also found in epileptic circuits (Clemens, 2004).

Therefore, probing how functional networks and theta oscillations are altered in WM processing and the relationship among them may help understand cognitive dysfunction in the epilepsy brain.

Significance

Working memory (WM) processing comprises emergent properties of neural oscillations and large-scale network interactions. The alteration of the interaction among these networks may be one key element in epilepsy with WM dysfunction. Here, we found there was widespread decreased deactivation in idiopathic generalized epilepsy (IGE) during WM, and the counteraction between the activation network and deactivation network was changed. Moreover, the correlation with frontal theta power indicated the unbalance of the counteraction between the activation and deactivation networks disturbed the efficiency of the WM process in IGE.

In this study, we used simultaneous EEG and fMRI to examine the features of neural oscillation and functional connectivity during the n-back WM task in patients with IGE. The theta power in frontal electrodes was calculated, and fMRI activations/deactivations correlated with n-back tasks were estimated. Moreover, functional connectivity dependent on the WM task among activation and deactivation networks was examined using a psychophysiological interaction (PPI) (Friston et al., 1997), which aimed to detect the coupling of one region to another with the modulation of other experimental or intrinsic factors. Finally, the relationship between theta features and WM-related functional connectivity in epilepsy was investigated.

2 | MATERIALS AND METHODS

2.1 | Participants

Thirty-two patients with IGE were recruited in this study (16 females; mean age: 27 years) from the Sichuan Provincial People's Hospital. Diagnosis and classification were made by the neurologists in accordance with the International League Against Epilepsy (ILAE) guidelines (Fisher et al., 2017; Scheffer et al., 2017) combined with the results of the routine EEG, CT, and MRI examinations. All the patients in this study were characterized by generalized tonic–clonic seizures (GTCS), and no structural abnormalities were found in any of the epilepsy patients. Thirty-two age- and gender-matched healthy controls (21 females; mean age: 23.3 years) with no history of psychiatric or neurologic disorders were socially recruited in the study. The demographics of the patients and healthy controls are shown in Tables 1 and 2. Written informed consent according to the Declaration of Helsinki was obtained from all participants. This study was approved by the Ethics Committee of the University of Electronic Science and Technology of China (UESTC).

TABLE 1 Summary of demographics of patients and healthy controls.

	HC		Patients		χ^2/t-test	
	n = 33		n = 32		p-value	
Gender (male/female)	12/21		16/16		.375	
Seizure type	–		GTCS		–	
	Mean	Std	Mean	Std		
Age (years)	23.3	2.4	25	5.7	0.074	
Seizure duration	–	–	5.3	5.6	–	–
Age at seizure onset	–	–	19.8	6.3	–	–

2.2 | Stimuli and task

Participants performed a visual n-back WM task with two memory loads, that is, 1-back and 2-back. Here, we used a block-design paradigm to separate the task effects. Instructions and a short practice were given outside the scanner before scanning. There were also verbal instructions at the beginning of each run. Two runs were conducted for each participant. In each block, lists of stimuli with three kinds of shapes (square, circle, triangle) were presented in a pseudorandom order. Each run consisted of a resting period of 10 s and a screen tip of 4 s, immediately followed by six blocks, with an interblock interval of 14 s. Each 1-back block lasted 44 s, within which 11 stimuli were presented one at a time (2500 ms of exposure time for each stimulus) with an interstimulus interval of 1500 ms. Each 2-back block lasted 48 s with 12 stimuli presented, with 2500 ms of exposure time for each stimulus and 1500 ms of interstimulus interval. Participants were instructed to pay attention to a sequence of visual stimuli and press two predefined buttons responding after each stimulus. In the 1-back task, participants pressed the right button with the right thumb finger whenever the stimulus was the same as the previous one, while pressed the left button with the left thumb whenever the stimulus was different from the previous one. In the 2-back task, participants press the right button whenever the stimulus was the same as that presented two back, and if the stimulus was different, participants were instructed to press the left button. In the resting periods, participants were told to remain still and pay attention to a fixation point without any response. The experimental procedure is shown in Figure 1.

2.3 | Simultaneous EEG-fMRI acquisition

FMRI data in the condition of WM tasks were acquired using a 3T MRI scanner (Discovery MR750, GE) with an eight-channel-phased array head coil and gradient-echo planar imaging sequences (FOV = 24×24 cm^2, FA = 90°, TR/TE = 2000 ms/30 ms, matrix = 64×64, slice thickness/gap = 4 mm/0.4 mm). High-resolution T1-weighted images were also acquired using a 3D fast spoiled gradient echo (T1-3D FSPGR) sequence (FOV = 25.6×25.6 cm^2,

FA = 9°, matrix = 256×256, TR/TE = 5.936 ms/1.956 ms, slice thickness = 1 mm, no gap, 152 slices).

Simultaneous EEG in the condition of WM tasks was recorded using an MR-compatible EEG cap (64-channel, Neuroscan, Charlotte, NC). Electrodes were placed according to the 10–20 standard system. Before recording, Fcz was the recording reference, and electrode impedances were lowered to below 10 kΩ. The amplifier was settled outside the scanning room, and the sampling rate was set at 5000 Hz. Synchronization between the MR scanner's internal clock and the EEG recording facilitated artifact removal in EEG preprocessing.

2.4 | EEG-fMRI data preprocessing

FMRI data were preprocessed using SPM12 (http://www.fil.ion.ucl.ac.uk/spm/). The first five volumes were discarded from all fMRI scans for magnetization equilibrium. The remaining volumes were slice-timing corrected and spatially realigned. Individual T1 images were coregistered to the functional images and segmented and normalized to the Montreal Neurological Institute (MNI) space. All subjects had <1 mm for head movement and 1° for head rotation during MRI scanning, and there was no head motion difference between the two groups. Then, the functional images were spatially normalized based on the T1 transformation matrix, resampled to 3×3×3 mm^3 voxels, and spatially smoothed using a 6-mm full-width half-maximum Gaussian kernel. Nuisance signals (12 motion parameters, linear drift signals, and mean white matter and cerebrospinal fluid signals) were regressed out for the fMRI data.

Curry 7 software (Compumedics Neuroscan) was used to correct MR gradient artifacts and ballistocardiogram (BCG) artifacts. The gradient artifacts were removed via the template subtraction method using the triggers delivered from the MR scanner (Allen et al., 2000). Bandpass filtering (0.5–45 Hz) was performed, followed by downsampling to 250 Hz. Then, BCG artifacts were removed using the optimal basis set–based method according to the ECG channel (Niazy et al., 2005). Finally, the preprocessed EEGs were re-referenced to the neutral infinite reference using the reference electrode standardization technique (Yao, 2001).

2.5 | Spectral analysis of theta rhythm

Spectral analysis was conducted on the preprocessed EEG by the Matlab-based programs. As theta oscillation was widely considered to be related to WM processing, we focused on the frontoparietal electrodes, including F3, F4, C3, C4, CP1, and CP2, and extracted the power of theta rhythm (4–8 Hz). The averaged theta power spectral density (PSD) in the 1-back blocks and 2-back blocks was calculated based on Welch's modified periodogram method with a Hamming window tapering of 1 s length (Unde & Shriram, 2014; Welch, 1967). In addition, to examine the effect arising from the WM

TABLE 2 Clinical demographics of patient.

Patient	Female/male	Age	Age of seizure onset	Duration	AEDs	Education	Total IEDs events, n
sub01	M	30	20	10	VPA	H	0
sub02	M	31	24	7	VPA+CBZ	U	5
sub03	F	20	16	4	LEV	U	4
sub04	M	31	26	5	/	H	1
sub05	M	25	20	5	/	U	0
sub06	M	32	26	6	VPA+LTG	H	1
sub07	M	30	30	0	/	U	0
sub08	M	13	11	2	/	P	3
sub09	M	18	16	2	/	H	0
sub10	M	21	17	4	VPA	H	0
sub11	F	25	14	11	LTG	H	1
sub12	F	27	17	10	LEV	H	4
sub13	F	27	12	15	LEV	U	1
sub14	M	32	12	20	OCB	U	4
sub15	F	18	17	1	/	H	2
sub16	F	30	30	0	/	H	0
sub17	F	27	26	1	VPA+LTG	U	0
sub18	M	33	33	0	/	H	1
sub19	M	16	15	1	/	H	2
sub20	F	31	22	9	LTG	U	0
sub21	M	20	19	1	VPA	H	4
sub22	F	26	26	0	CBZ+OCB	P	0
sub23	F	30	22	8	CBZ	U	0
sub24	M	21	21	0	/	U	0
sub25	F	16	12	4	OCB	H	0
sub26	F	24	23	1	/	U	0
sub27	M	26	19	7	VPA	P	0
sub28	M	32	32	0	/	P	0
sub29	M	31	10	21	VPA+CBZ	H	0
sub30	M	23	15	8	LTG	P	3
sub31	F	22	15	7	LTG	U	0
sub32	F	18	17	1	LTG	H	0

Abbreviations: AEDs, antiepileptic drugs; CBZ, carbamazepine; F, female; H, high school; LEV, levetiracetam; LTG, lamotrigine; M, male; OCB, oxcarbazepine; P, primary school or junior school; U, university or college; VPA, valproic acid.
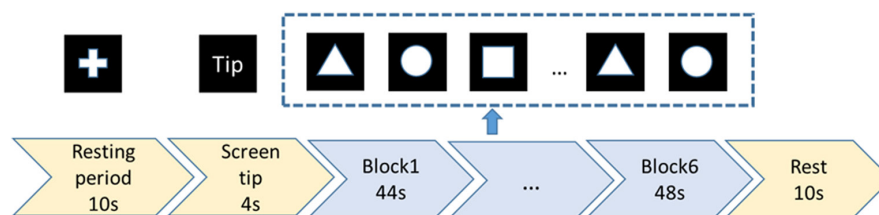

FIGURE 1 Working memory experimental protocol used in the current study.

load, theta change in tasks relative to the baseline (theta PSD in n-back minus that in the resting state at the interblock interval) was calculated. Then, we used repeated-measures ANOVAs to detect the group main effect, the task main effect, and the interaction effect of absolute theta PSD and the theta PSD increase in frontoparietal electrodes.

2.6 | fMRI activation analysis

Whole-brain statistical analysis of fMRI data was performed using the generalized linear model (GLM). For the first-level analysis, task-related fMRI activations and deactivations (negative activations) in a single subject were calculated. The stimuli variations of n-back tasks were convolved with the standard hemodynamic response function and then used as regressors in the GLM. The response during 1-back blocks was subtracted from that during the 2-back blocks. Then, the second-level analysis was conducted using the statistical images resulting from single-subject contrasts to examine the activation effect of 2-back conditions at the within-group (one-sample t-test) and between-group (two-sample t-test) levels.

2.7 | Psychophysiological interaction analysis

PPI analysis aimed to identify the contribution of one region to another with the modulation of experimental factors. The PPI model included correlation PPI terms, that is, psychological variables and physiological variables, and modulatory interaction terms. In this study, PPI analysis was performed based on the regions that represented significant between-group differences in the WM-related fMRI activation maps. The regions with significant differences ($p < .01$) were selected as the regions of interest (ROIs, 3 * 3 * 3 voxels), and the mean BOLD signals within the ROIs were extracted for each participant. Then, the connections among these ROIs depending on the 2-back condition were analyzed using the PPI model to detect the potential interaction effect between ROIs in the modulation of the 2-back task. Here, X_{r1} and Y_{r2} are the averaged BOLD signals of the two selected ROIs. We constructed the psychological regressor (X_{task}) as the stimulus under 2-back conditions. The interaction term (X_{int}) was the point-by-point multiplication between the psychological signal and the physiological signal, that is, $X_{r1\_dconv} \cdot X_{task}$, where the physiological regressor X_{r1_dconv} was the estimate of neural activity derived by deconvolution of HRF from the BOLD time series. Therefore, the significant coupling effect (β_{int}) can be considered the task-modulated functional connectivity from region 1 ($r1$) to region 2 ($r2$). Therefore, positive modulation effects denoted increased functional coupling modulated by the task from $r1$ to $r2$, while negative modulation effects denoted decreased functional coupling from $r1$ to $r2$.

$$Y_{r2} = \beta_0 + \beta_1 X_{r1} + \beta_{task}(X_{task} \cdot HRF) + \beta_{int}(X_{int} \cdot HRF)$$

2.8 | Statistical analysis

Before the between-group comparison and the correlation analysis, the normalization of the brain variables has been examined using the Shapiro–Wilk test. For the demographic information, the chi-square test was used for the comparison of gender, and age was compared using the two-sample t-test after we checked the normalization of the data. Then, we used repeated-measures ANOVAs to detect the group main effect, the task main effect, and the interaction effect of absolute theta PSD and the theta PSD increase in frontoparietal electrodes. In addition, the frontal theta power, that is, the sum of the F3 and F4 PSD, was correlated with the behavior measurement (the response time [RT] and accuracy) during WM tasks. For the fMRI data, the activation effects were obtained based on two-level analysis. The statistical maps were corrected for multiple comparisons with false discovery rate (FDR) calculation. Moreover, after PPI analysis, the comparison of task-modulated functional connectivity was conducted between groups (two-sample t-test). In the between-group comparison, age, gender, and education years were regressed as the covariates. Finally, the relationship between fMRI features and frontal theta power in the condition of the 2-back task in IGE patients was examined. Here, the frontal theta power was the averaged theta PSD in F3 and F4 in this condition. The activation in ROI and PPI connections between ROIs that were significantly altered in the IGE group were extracted, and then, Pearson's correlation analysis was performed with the theta PSD in the 2-back task. The statistical analysis was conducted based on the Matlab-based program.
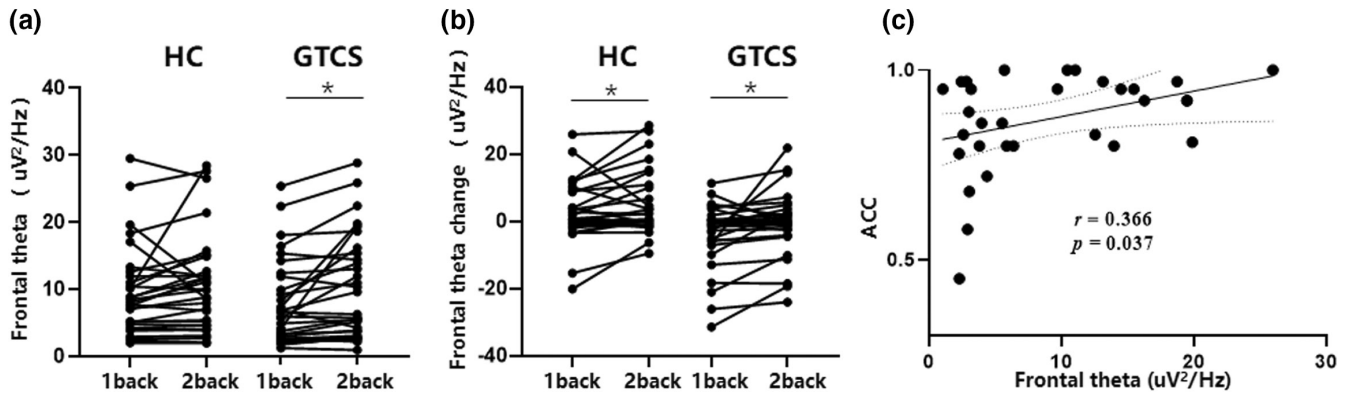
3 | RESULTS

3.1 | Group-level analysis of behavior data

The RT and accuracy (ACC) in the n-back tasks were submitted to repeated-measures ANOVAs and post-hoc t-tests. At the within-group level, the IGE group showed increased RT and decreased ACC with increasing memory load ($p < .001$), while there was no significant difference between the 1-back and 2-back tasks in HC. Compared with the HC group, the IGE group demonstrated a significant decrease in ACC in the 2-back task and an increase in RT in the 1-back task ($p < .05$). An interaction effect was found for both RT and ACC between the group and WM load ($p < .001$ for ACC, and $p = .052$ for RT). The average ACC in 2-back task in epilepsy was 0.86. In addition, in the epilepsy group, the behavior data were correlated with age, rather with the education years, the duration of epilepsy seizure, or the antiepileptic drug use.

3.2 | Results of theta spectral analysis

The results showed that there was a significant task effect of the absolute theta PSD at frontal electrodes (average theta PSD of F3, F4 electrode) in GTCS ($p < .05$) (Figure 2a). Then, we calculated the theta power change in different levels of WM tasks relative to the resting state, and the results showed both GTCS and HC groups had greater theta increase in 2-back task compared with 1-back task (Figure 2b). That is, the increase in WM load was accompanied by the significant enhancement of frontal theta PSD. Moreover, group-level main effect was found, and theta PSD increase was

FIGURE 2 The results of the frontal theta power in different conditions. (a) GTCS showed that the increase in working memory load was accompanied by the significant enhancement of theta PSD. (b) Both GTCS and HC showed larger theta PSD change in 2-back task compared with that in 1-task. Moreover, a significant difference was demonstrated between idiopathic generalized epilepsy (IGE) and HC. (c) Positive correlation between frontal theta PSD and the accuracy index during WM processing. The black star means the statistical significance $p < .05$; Frontal theta: the averaged theta power spectral density (PSD) at F3 and F4; Frontal theta change: the averaged theta PSD change at F3 and F4 relative to the resting state; ACC: accuracy during working memory tasks.

much larger in HC than that in the GTCS group. The spectral analysis was also conducted at a single electrode, and the results were shown in Figures S1 and S2. However, neither group effect nor task effect was found for theta PSD change in parietal electrodes, that is, C3, C4, CP1, and CP2. In addition, we calculated the correlation between the frontal theta power with the behavior measurement, and a positive correlation with the ACC in 2-back tasks was found (Figure 2c).

3.3 | fMRI activations and deactivations related to the 2-back task

We calculated the brain activation maps correlated with the n-back WM task in epilepsy patients and HCs. The results of comparisons within groups and between groups are shown in Figure 3. In both the HC and IGE groups, the task activations correlated with n-back tasks were dominant in the frontoparietal network, while the task activations involved the DMN, the primary visual, auditory and motor cortices, and the cerebellum. Moreover, more activation in the frontoparietal network occurred with increasing WM load. In the 2-back>1-back contrast, there were higher and broader activations in frontoparietal areas, as well as a few increased deactivations in DMN areas, mainly in the middle and post-cingulate cortex. Here, we defined the frontoparietal regions that represented activations in the 2-back task as the WMN, including the supp_motor_area (SMA), frontal_sup, frontal_mid, parietal_sup, and parietal_inf areas. Compared with HCs, there were much wider activation areas in both 1-back and 2-back tasks in IGE, while the deactivation areas diminished greatly. With the WM load increasing, widespread decreased deactivations were found in IGE compared with HC, including the areas in WMN, DMN, and occipital/temporal areas ($p < .001$, two-sample t-test, Figure 4 and Table 3). These brain areas that demonstrated significant alterations in IGE were selected as ROIs for the following PPI analysis.

### 3.4 | Psychophysiological interaction network results

The directed network among ROIs that was dependent on 2-back tasks was constructed based on PPI analysis. Here, ROIs were selected demonstrating significant alteration of activations/deactivations in IGE (here, the threshold was set as $p < .01$). Compared with HCs, decreased positive connectivity was located among the deactivation regions in IGE, including the DMN and occipital and temporal areas. Moreover, IGE showed decreased negative connectivity between frontal WMN areas and the deactivation networks, such as the occipital area and the middle cingulum. The significant group-level connections based on PPI analysis are shown in Figure 5.

3.5 | Correlation between theta feature and task-dependent network features

Correlation between theta power and PPI connectivity, as well as the fMRI activations in ROIs depending on 2-back tasks, was performed. The result is shown in Figure 5. It was found that the fMRI activations in WMN regions, that is, frontal_sup_medial and SMA, were accompanied by increased frontal theta power. In addition, the increased negative connectivity between these WMN regions and occipital regions was accompanied by increased frontal theta power.

4 | DISCUSSION

This study investigated EEG and fMRI representations related to the n-back WM task. The enhancement of frontal theta power was accompanied by an increase in WM load and behavior accuracy in IGE. Moreover, fMRI activations were demonstrated in the WMN
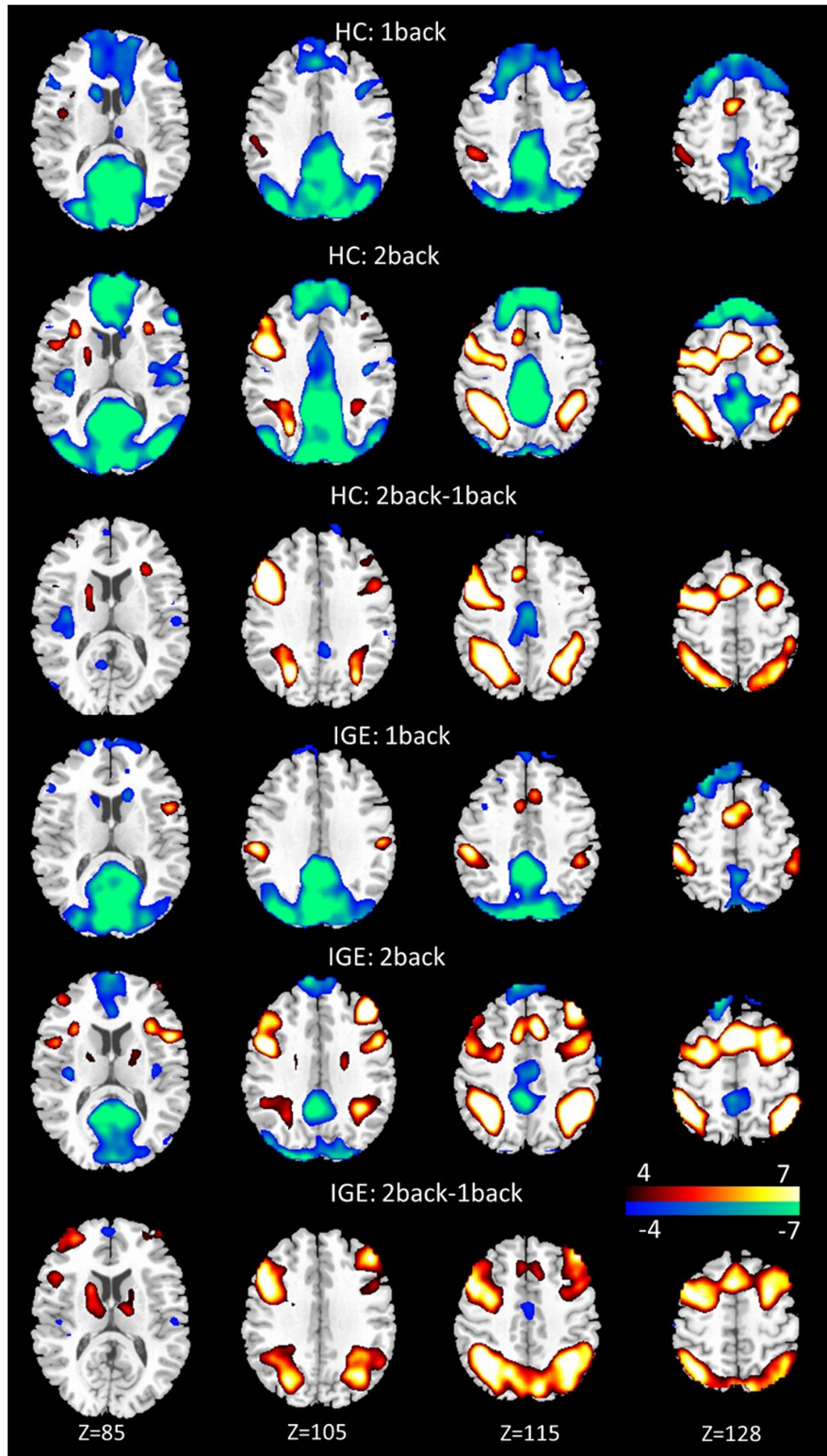
FIGURE 3 Brain activation maps correlated with the n-back working memory task in epilepsy patients and HCs. Widespread activation was found in idiopathic generalized epilepsy in different conditions of working memory processing.

during n-back tasks, while the IGE group showed more decreased deactivations in DMN, and primary visual and auditory network. In addition, the functional connectivity among these regions dependent on the 2-back task was constructed using PPI analysis, and decreased negative connectivity both within the frontal activation network and deactivation network, as well as decreased positive connectivity between the activation network and deactivation network, was found. Finally, the relationship with frontal theta power
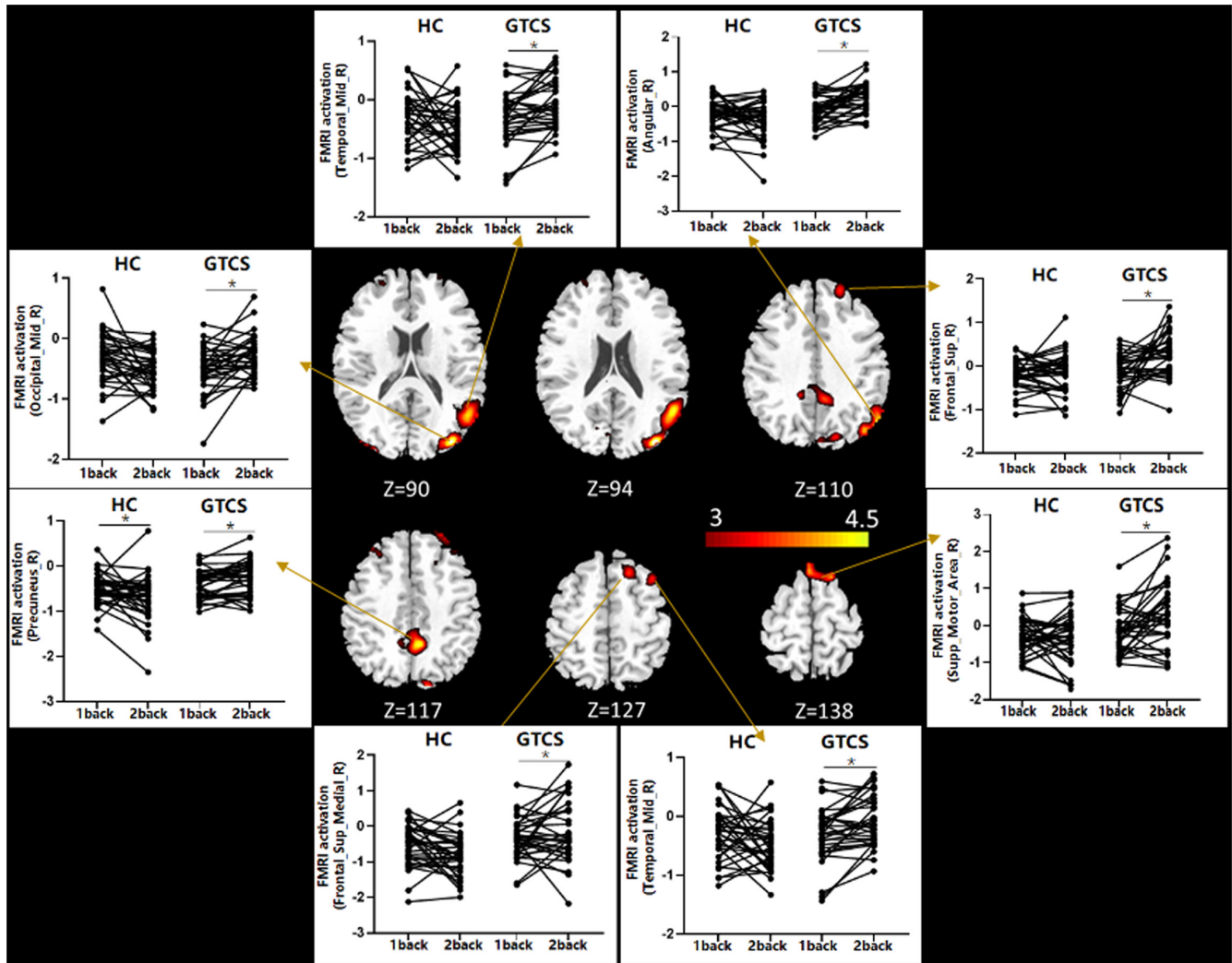
FIGURE 4 The between-group result (IGE-HC) of the fMRI activation correlated with 2-back>1-back contrast ($p < .05$, FDR-corrected). The hot colors are the brain area with less deactivation in IGE than HC. The bar charts demonstrated the fMRI activation for the regions of interest with a significant difference in between-group analysis. The GTCS group showed less deactivation and more activation during 2-back task compared with 1-back task.

TABLE 3 The between-group comparisons (IGE-HC) of brain activation maps correlated with 2-back>1-back contrast ($p < .001$).

Brain regions (AAL)	Montreal Neurological Institute coordinate (mm)			T-value	Cluster
	X	Y	Z		
Frontal_Sup_Medial_R	7	33	60	4.2712	28
Frontal_Sup_R	27	51	42	4.0451	24
Supp_Motor_Area_R	3	21	64	3.8675	19
Precuneus_R	6	−51	42	4.3715	45
Cuneus_R	14	−69	27	4.0585	20
Angular_R	53	−61	30	4.0575	106
Occipital_Mid_R	36	−87	18	4.8453	90
Temporal_Mid_R	51	−61	18	4.1643	67

Note: The anatomical names of these AAL regions were described in the Table S1.

indicated that the unbalance of the anticorrelation between the activation and deactivation networks disturbed the efficiency of the WM process in IGE.

Theta oscillations are widely found in many cognitive activities and are involved in the allocation of attention, attention control, and directing local and long-range activity during information processing
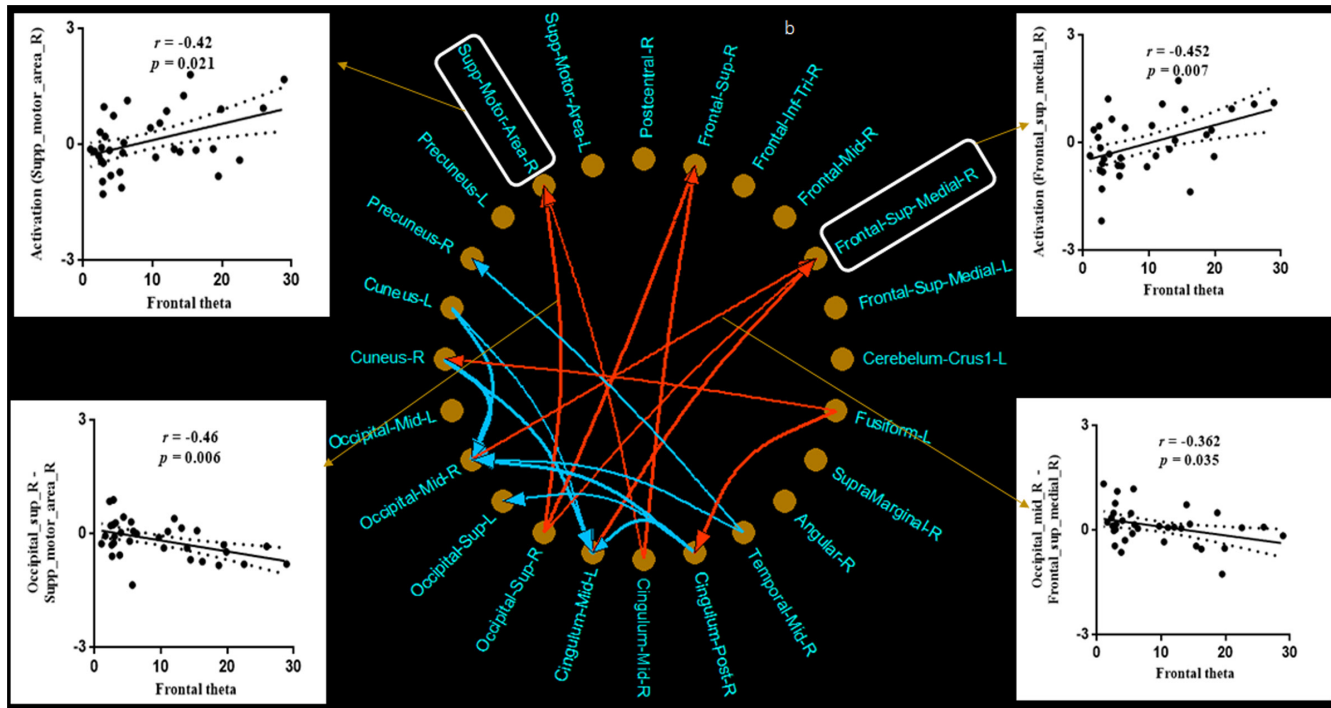
FIGURE 5 Group-level results of psychophysiological interaction (PPI) connections dependent on the 2-back working memory (WM) task. The subgraph in the middle is the two-sample *t*-test result of PPI connections between idiopathic generalized epilepsy (IGE) and HC. The red line denotes decreased negative coupling, and the blue line denotes decreased positive coupling in the IGE. The subgraphs around are the correlation results between frontal theta PSD in the 2-back WM task and fMRI activation, as well as PPI connections. Occipital_mid_R-Frontal_sup_medial_R: the PPI connection between the occipital_mid_R area and the frontal_sup_medial_R area; Occipital_sup_R-Supp_motor_area_R: the PPI connection between the occipital_sup_R area and the supplementary motor area.

(Missonnier et al., 2006; Ward, 2003). In WM tasks, the power and connectivity of the theta band were enhanced, accompanied by the highly increased synchronization of theta rhythm (Itthipuripat et al., 2013). In the current study, increased theta power in frontal electrodes was demonstrated in the 2-back task compared with the 1-back task. The activity of frontal theta during the period of WM played a positive role with the increasing demand for attention and central execution (Jensen & Tesche, 2002). Moreover, theta PSD increase was much larger in HC than that in the GTCS group. These results indicated that the enhancement of theta oscillation was necessary for increasing WM load, while in IGE, the positive correlation with the ACC in 2-back tasks suggested much more effort may be needed to facilitate resource allocation and information processing in high-load WM tasks.

Previous studies showed that theta-related networks in WM directed the information flowing from the frontal to other brain regions (Honey et al., 2002; Klingberg et al., 2002; Nee & Brown, 2013), and WM capacity was enhanced by distributed prefrontal activation (Tang et al., 2019). As the current study showed, the fMRI activations correlated with n-back tasks involved distributed frontal and parietal areas, while deactivation in DMN and primary visual/auditory networks was also demonstrated. Moreover, with the increasing WM load, much higher and broader activations in frontoparietal areas were found. That is, the increasing resources required in the high-level WM task made some areas in deactivation networks,

such as the DMN, convert to activation areas. The results were consistent with previous common findings (Koshino et al., 2005; Vu et al., 2013). While in epilepsy, abnormal brain activation and connectivity have been demonstrated in patients with focal epilepsy (Lv et al., 2014; Stretton et al., 2012), and higher ERP amplitude was found in idiopathic epilepsy compared with the control group over frontal and central regions (Myatchin et al., 2009). In the current study, increased activation and diminished deactivation in IGE implied the abnormality of resource mediation of WM processing. The decreased deactivation of the DMN may be related to the inefficient balance and regulation of introspective and exterior input processing in tasks in epilepsy.

This study used the PPI model to detect functional connectivity dependent on WM tasks. Anticorrelation between the frontoparietal network and default networks supported goal-directed cognition and WM processes (Piccoli et al., 2015; Spreng et al., 2010). This counteraction between the activation network and deactivation network may be associated with top-down processing, serving as the cortical mediator linking introspective and exterior input processing (Xin & Lei, 2015). On the other hand, aberrant functional connectivity in epilepsy has been widely reported in thalamocortical circuits and widespread cortical networks, such as the frontal central execution network, sensorimotor network, and DMN (Clemens et al., 2013; Jiruska et al., 2013). In this study, decreased negative coupling between frontal activation areas

and deactivation areas was found in epilepsy, which indicated an unbalance between the task-positive network and task-negative network. The decreased positive connectivity within deactivation areas may also be associated with the extended activation and the decreased deactivation, which implies the reallocation of WM resources in epilepsy. Moreover, the negative relationship between disturbed connectivity and frontal theta power also illuminated the role of the counteraction between the activation network and deactivation network on the information processing and resource allocation underlying enhanced cognition (Solomon et al., 2017). The disrupted anticorrelation and the decreased theta power may be indicators of abnormal WM function suffering from long-term epileptic activity.

There are several limitations in this study. First, the interictal epileptic discharges (IEDs) during fMRI scanning may have a significant impact on the results. Therefore, we examined the correlation between the number of IED events during fMRI scanning and the behavior data. It was shown that there was a correlation between the IEDs and the RT of 1-back WM task, suggesting the disturbance of the discharges on the low-load cognitive function. Second, the relationship between local theta oscillations and functional connectivity was investigated; however, more in-depth exploration of the causality among them and their role in modulating WM processing is needed in future studies. Third, as the WM tasks represented summarization of the attention, memory, and execution function, the cognitive impairment, as well as the antiepileptic drug may affect the performance in WM tasks. Therefore, combining the brain features with the behavior and the clinical evaluations would be helpful for uncovering the impairment of cognition in the epileptic brain. Moreover, the sample size is relatively small in this study, and future studies should include a larger sample to determine the mechanism underlying the cognitive impairment of epilepsy.

5 | CONCLUSION

This study investigated the relationship between EEG and fMRI-based activation, as well as the functional connectivity in the n-back WM task. Enhancement of the activations in the frontal activation network, DMN, and the primary network was found in IGE. In addition, the functional connectivity using PPI analysis demonstrated altered connectivity among the activation and deactivation networks in IGE. Our findings demonstrated the unbalance of the interactions between activation and deactivation networks during the WM process in IGE, and the correlation with theta power may indicate the pathophysiological mechanism of WM dysfunction in epilepsy.

DECLARATION OF TRANSPARENCY

The authors, reviewers and editors affirm that in accordance to the policies set by the *Journal of Neuroscience Research*, this manuscript presents an accurate and transparent account of the study being reported and that all critical details describing the methods and results are present.

AUTHOR CONTRIBUTIONS

YQ: conceptualization, methodology, investigation, data curation, formal analysis, visualization, writing - first draft, writing - review & editing. SJ: conceptualization, validation, writing - review & editing. SX: methodology, investigation, data curation. SL: methodology, investigation, data curation. QF: methodology, investigation, data curation. LY: conceptualization, investigation. PD: conceptualization, investigation. CL: conceptualization, validation, supervision, writing - review & editing. DY: conceptualization, validation, supervision.

CONFLICT OF INTEREST STATEMENT

None of the authors have a conflict of interest to disclose.

PEER REVIEW

The peer review history for this article is available at https://publons.com/publon/10.1002/jnr.25183.

DATA AVAILABILITY STATEMENT

The data that support the findings of this study are available from the corresponding author upon request.

ORCID

Yun Qin 🅙 https://orcid.org/0000-0002-8106-6137
Lili Yang 🅙 https://orcid.org/0000-0002-3054-3044

REFERENCES

Allen, P. J., Josephs, O., & Turner, R. (2000). A method for removing imaging artifact from continuous EEG recorded during functional MRI. *Neuroimage*, *12*(2), 230–239. https://doi.org/10.1006/nimg.2000.0599

Bai, X., Vestal, M., Berman, R., Negishi, M., Spann, M., Vega, C., Desalvo, M., Novotny, E. J., Constable, R. T., & Blumenfeld, H. (2010). Dynamic time course of typical childhood absence seizures: EEG, behavior, and functional magnetic resonance imaging. *Journal of Neuroscience*, *30*(17), 5884–5893. https://doi.org/10.1523/JNEUROSCI.5101-09.2010

Buzsaki, G., & Draguhn, A. (2004). Neuronal oscillations in cortical networks. *Science*, *304*(5679), 1926–1929. https://doi.org/10.1126/science.1099745

Clemens, B. (2004). Pathological theta oscillations in idiopathic generalised epilepsy. *Clinical Neurophysiology*, *115*(6), 1436–1441. https://doi.org/10.1016/j.clinph.2004.01.018

Clemens, B., Puskas, S., Besenyei, M., Spisak, T., Opposits, G., Hollody, K., Fogarasi, A., Fekete, I., & Emri, M. (2013). Neurophysiology of juvenile myoclonic epilepsy: EEG-based network and graph analysis of the interictal and immediate preictal states. *Epilepsy Research*, *106*(3), 357–369. https://doi.org/10.1016/j.eplepsyres.2013.06.017

Cohen, J. D., Perlstein, W. M., Braver, T. S., Nystrom, L. E., Noll, D. C., Jonides, J., & Smith, E. E. (1997). Temporal dynamics of brain activation during a working memory task. *Nature*, *386*(6625), 604–608. https://doi.org/10.1038/386604a0

Deiber, M. P., Missonnier, P., Bertrand, O., Gold, G., Fazio-Costa, L., Ibanez, V., & Giannakopoulos, P. (2007). Distinction between perceptual and attentional processing in working memory tasks: A study of phase-locked and induced oscillatory brain dynamics. *Journal of Cognitive Neuroscience*, *19*(1), 158–172. https://doi.org/10.1162/jocn.2007.19.1.158

Fisher, R. S., Cross, J. H., French, J. A., Higurashi, N., Hirsch, E., Jansen, F. E., Lagae, L., Moshé, S. L., Peltola, J., Perez, E. R., Scheffer, I. E., & Zuberi, S. M. (2017). Operational classification of seizure types by the international league against epilepsy: Position paper of the ILAE Commission for Classification and Terminology. *Epilepsia*, *58*(4), 522–530. https://doi.org/10.1111/epi.13670

Friston, K. J., Buechel, C., Fink, G. R., Morris, J., Rolls, E., & Dolan, R. J. (1997). Psychophysiological and modulatory interactions in neuroimaging. *Neuroimage*, *6*(3), 218–229. https://doi.org/10.1006/nimg.1997.0291

Gotman, J., Grova, C., Bagshaw, A., Kobayashi, E., Aghakhani, Y., & Dubeau, F. (2005). Generalized epileptic discharges show thalamocortical activation and suspension of the default state of the brain. *Proceedings of the National Academy of Sciences of the United States of America*, *102*(42), 15236–15240. https://doi.org/10.1073/pnas.0504935102

Honey, G. D., Fu, C. H. Y., Kim, J., Brammer, M. J., Croudace, T. J., Suckling, J., Pich, E. M., Williams, S. C. R., & Bullmore, E. T. (2002). Effects of verbal working memory load on corticocortical connectivity modeled by path analysis of functional magnetic resonance imaging data. *Neuroimage*, *17*(2), 573–582. https://doi.org/10.1006/nimg.2002.1193

Hsieh, L. T., & Ranganath, C. (2014). Frontal midline theta oscillations during working memory maintenance and episodic encoding and retrieval. *Neuroimage*, *85*, 721–729. https://doi.org/10.1016/j.neuroimage.2013.08.003

Itthipuripat, S., Wessel, J. R., & Aron, A. R. (2013). Frontal theta is a signature of successful working memory manipulation. *Experimental Brain Research*, *224*(2), 255–262. https://doi.org/10.1007/s00221-012-3305-3

Jensen, O., & Tesche, C. D. (2002). Frontal theta activity in humans increases with memory load in a working memory task. *European Journal of Neuroscience*, *15*(8), 1395–1399. https://doi.org/10.1046/j.1460-9568.2002.01975.x

Jiruska, P., de Curtis, M., Jefferys, J. G., Schevon, C. A., Schiff, S. J., & Schindler, K. (2013). Synchronization and desynchronization in epilepsy: Controversies and hypotheses. *Journal of Physiology*, *591*(4), 787–797. https://doi.org/10.1113/jphysiol.2012.239590

Johnson, E. L., Adams, J. N., Solbakk, A. K., Endestad, T., Larsson, P. G., Ivanovic, J., Meling, T. R., Lin, J. J., & Knight, R. T. (2018). Dynamic frontotemporal systems process space and time in working memory. *PLoS Biology*, *16*(3), e2004274. https://doi.org/10.1371/journal.pbio.2004274

Klimesch, W. (1999). EEG alpha and theta oscillations reflect cognitive and memory performance: A review and analysis. *Brain Research Reviews*, *29*(2–3), 169–195. https://doi.org/10.1016/S0165-0173(98)00056-3

Klingberg, T., Forssberg, H., & Westerberg, H. (2002). Increased brain activity in frontal and parietal cortex underlies the development of visuospatial working memory capacity during childhood. *Journal of Cognitive Neuroscience*, *14*(1), 1–10. https://doi.org/10.1162/089892902317205276

Klingberg, T., O'Sullivan, B. T., & Roland, P. E. (1997). Bilateral activation of fronto-parietal networks by incrementing demand in a working memory task. *Cerebral Cortex*, *7*(5), 465–471. https://doi.org/10.1093/cercor/7.5.465

Koshino, H., Carpenter, P. A., Minshew, N. J., Cherkassky, V. L., Keller, T. A., & Just, M. A. (2005). Functional connectivity in an fMRI working memory task in high-functioning autism. *Neuroimage*, *24*(3), 810–821. https://doi.org/10.1016/j.neuroimage.2004.09.028

Koshino, H., Minamoto, T., Yaoi, K., Osaka, M., & Osaka, N. (2014). Coactivation of the default mode network regions and working memory network regions during task preparation. *Scientific Reports*, *4*, 5954. https://doi.org/10.1038/Srep05954

Lee, C., Kim, S. M., Jung, Y. J., Im, C. H., Kim, D. W., & Jung, K. Y. (2014). Causal influence of epileptic network during spike-and-wave discharge in juvenile myoclonic epilepsy. *Epilepsy Research*, *108*(2), 257–266. https://doi.org/10.1016/j.eplepsyres.2013.11.005

Luo, C., Li, Q., Lai, Y., Xia, Y., Qin, Y., Liao, W., Li, S., Zhou, D., Yao, D., & Gong, Q. (2011). Altered functional connectivity in default mode network in absence epilepsy: A resting-state fMRI study. *Human Brain Mapping*, *32*(3), 438–449. https://doi.org/10.1002/hbm.21034

Lv, Z. X., Huang, D. H., Ye, W., Chen, Z. R., Huang, W. L., & Zheng, J. O. (2014). Alteration of functional connectivity within visuospatial working memory-related brain network in patients with right temporal lobe epilepsy: A resting-state fMRI study. *Epilepsy & Behavior*, *35*, 64–71. https://doi.org/10.1016/j.yebeh.2014.04.001

Missonnier, P., Deiber, M. P., Gold, G., Millet, P., Pun, M. G. F., Fazio-Costa, L., Giannakopoulos, P., & Ibanez, V. (2006). Frontal theta event-related synchronization: Comparison of directed attention and working memory load effects. *Journal of Neural Transmission*, *113*(10), 1477–1486. https://doi.org/10.1007/s00702-005-0443-9

Myatchin, I., Mennes, M., Wouters, H., Stiers, P., & Lagae, L. (2009). Working memory in children with epilepsy: An event-related potentials study. *Epilepsy Research*, *86*(2–3), 183–190. https://doi.org/10.1016/j.eplepsyres.2009.06.004

Nee, D. E., & Brown, J. W. (2013). Dissociable frontal-striatal and frontal-parietal networks involved in updating hierarchical contexts in working memory. *Cerebral Cortex*, *23*(9), 2146–2158. https://doi.org/10.1093/cercor/bhs194

Newton, A. T., Morgan, V. L., Rogers, B. P., & Gore, J. C. (2011). Modulation of steady state functional connectivity in the default mode and working memory networks by cognitive load. *Human Brain Mapping*, *32*(10), 1649–1659. https://doi.org/10.1002/hbm.21138

Niazy, R. K., Beckmann, C. F., Iannetti, G. D., Brady, J. M., & Smith, S. M. (2005). Removal of FMRI environment artifacts from EEG data using optimal basis sets. *NeuroImage*, *28*(3), 720–737. https://doi.org/10.1016/j.neuroimage.2005.06.067

Piccoli, T., Valente, G., Linden, D. E. J., Re, M., Esposito, F., Sack, A. T., & Di Salle, F. (2015). The default mode network and the working memory network are not anti-correlated during all phases of a working memory task. *PLoS ONE*, *10*(4), e0123354. https://doi.org/10.1371/journal.pone.0123354

Qin, Y., Jiang, S., Zhang, Q., Dong, L., Jia, X., He, H., Yao, Y., Yang, H., Zhang, T., Luo, C., & Yao, D. (2019). BOLD-fMRI activity informed by network variation of scalp EEG in juvenile myoclonic epilepsy. *NeuroImage: Clinical*, *22*, 101759. https://doi.org/10.1016/j.nicl.2019.101759

Rutishauser, U., Ross, I. B., Mamelak, A. N., & Schuman, E. M. (2010). Human memory strength is predicted by theta-frequency phase-locking of single neurons. *Nature*, *464*(7290), 903–907. https://doi.org/10.1038/nature08860

Santana, I., Lemos, R., Cunha, C., & Barbosa, V. (2006). Epilepsy and memory: Learning processing and working memory compromise in frontal lobe epilepsy. *Epilepsia*, *47*, 163.

Sarnthein, J., Morel, A., von Stein, A., & Jeanmonod, D. (2005). Thalamocortical theta coherence in neurological patients at rest and during a working memory task. *International Journal of Psychophysiology*, *57*(2), 87–96. https://doi.org/10.1016/j.ijpsycho.2005.03.015

Scheffer, I. E., Berkovic, S., Capovilla, G., Connolly, M. B., French, J., Guilhoto, L., Hirsch, E., Jain, S., Mathern, G. W., Moshé, S. L., Nordli, D. R., Perucca, E., Tomson, T., Wiebe, S., Zhang, Y.-H., & Zuberi, S. M. (2017). ILAE classification of the epilepsies: Position paper of the ILAE Commission for Classification and Terminology. *Epilepsia*, *58*(4), 512–521. https://doi.org/10.1111/epi.13709

Solomon, E. A., Kragel, J. E., Sperling, M. R., Sharan, A., Worrell, G., Kucewicz, M., Inman, C. S., Lega, B., Davis, K. A., Stein, J. M., Jobst, B. C., Zaghloul, K. A., Sheth, S. A., Rizzuto, D. S., & Kahana, M. J. (2017). Widespread theta synchrony and high-frequency desynchronization underlies enhanced cognition. *Nature Communications*, *8*, 1704. https://doi.org/10.1038/S41467-017-01763-2

Spreng, R. N., Stevens, W. D., Chamberlain, J. P., Gilmore, A. W., & Schacter, D. L. (2010). Default network activity, coupled with the frontoparietal control network, supports goal-directed cognition. *Neuroimage*, *53*(1), 303–317. https://doi.org/10.1016/j.neuroimage.2010.06.016

Sreenivasan, K. K., Curtis, C. E., & D'Esposito, M. (2014). Revisiting the role of persistent neural activity during working memory. *Trends in Cognitive Sciences*, *18*(2), 82–89. https://doi.org/10.1016/j.tics.2013.12.001

Stretton, J., Winston, G., Sidhu, M., Centeno, M., Vollmar, C., Ili, S. B., Symms, M., Koepp, M., Duncan, J. S., & Thompson, P. J. (2012). Neural correlates of working memory in temporal lobe epilepsy—An fMRI study. *Neuroimage*, *60*(3), 1696–1703. https://doi.org/10.1016/j.neuroimage.2012.01.126

Swartz, B. E., Simpkins, F., Halgren, E., Mandelkern, M., Brown, C., Krisdakumtorn, T., & Gee, M. (1996). Visual working memory in primary generalized epilepsy: An (18)FDG-PET study. *Neurology*, *47*(5), 1203–1212. https://doi.org/10.1212/Wnl.47.5.1203

Tang, H., Qi, X. L., Riley, M. R., & Constantinidis, C. (2019). Working memory capacity is enhanced by distributed prefrontal activation and invariant temporal dynamics. *Proceedings of the National Academy of Sciences of the United States of America*, *116*(14), 7095–7100. https://doi.org/10.1073/pnas.1817278116

Todd, J. J., & Marois, R. (2004). Capacity limit of visual short-term memory in human posterior parietal cortex. *Nature*, *428*(6984), 751–754. https://doi.org/10.1038/nature02466

Toth, B., Boha, R., Posfai, M., Gaal, Z. A., Konya, A., Stam, C. J., & Molnar, M. (2012). EEG synchronization characteristics of functional connectivity and complex network properties of memory maintenance in the delta and theta frequency bands. *International Journal of Psychophysiology*, *83*(3), 399–402. https://doi.org/10.1016/j.ijpsycho.2011.11.017

Unde, S. A., & Shriram, R. (2014). *Coherence analysis of EEG signal using power spectral density*. Fourth International Conference on Communication Systems and Network Technologies.

Vaudano, A. E., Laufs, H., Kiebel, S. J., Carmichael, D. W., Hamandi, K., Guye, M., Thornton, R., Rodionov, R., Friston, K. J., Duncan, J. S., & Lemieux, L. (2009). Causal hierarchy within the thalamo-cortical network in spike and wave discharges. *PLoS ONE*, *4*(8), e6475. https://doi.org/10.1371/journal.pone.0006475

Violante, I. R., Li, L. M., Carmichael, D. W., Lorenz, R., Leech, R., Hampshire, A., Rothwell, J. C., & Sharp, D. J. (2017). Externally induced frontoparietal synchronization modulates network dynamics and enhances working memory performance. *eLife*, *6*, e22001. https://doi.org/10.7554/elife.22001.001

Vu, M. A. T., Thermenos, H. W., Terry, D. P., Wolfe, D. J., Voglmaier, M. M., Niznikiewicz, M. A., McCarley, R. W., Seidman, L. J., & Dickey, C. C. (2013). Working memory in schizotypal personality disorder: fMRI activation and deactivation differences. *Schizophrenia Research*, *151*(1–3), 113–123. https://doi.org/10.1016/j.schres.2013.09.013

Ward, L. M. (2003). Synchronous neural oscillations and cognitive processes. *Trends in Cognitive Sciences*, *7*(12), 553–559. https://doi.org/10.1016/j.tics.2003.10.012

Welch, P. (1967). The use of fast Fourier transform for the estimation of power spectra: A method based on time averaging over short, modified periodograms. *IEEE Transactions on Audio and Electroacoustics*, *15*(2), 70–73.

Xin, F., & Lei, X. (2015). Competition between frontoparietal control and default networks supports social working memory and empathy. *Social Cognitive and Affective Neuroscience*, *10*(8), 1144–1152. https://doi.org/10.1093/scan/nsu160

Yao, D. Z. (2001). A method to standardize a reference of scalp EEG recordings to a point at infinity. *Physiological Measurement*, *22*(4), 693–711. https://doi.org/10.1088/0967-3334/22/4/305

Zakrzewska, M. Z., & Brzezicka, A. (2014). Working memory capacity as a moderator of load-related frontal midline theta variability in Sternberg task. *Frontiers in Human Neuroscience*, *8*, 399. https://doi.org/10.3389/Fnhum.2014.00399

SUPPORTING INFORMATION

Additional supporting information can be found online in the Supporting Information section at the end of this article.

FIGURE S1 The results of the frontal theta power in frontoparietal electrodes.

FIGURE S2 The results of the frontal theta change in frontoparietal electrodes.

TABLE S1 The abbreviations and the corresponding anatomical name of the brain regions in this study.

Transparent Science Questionnaire for Authors